Available online at www.sciencedirect.com
SCIENCE DIRECT®
Electrochimica Acta 50 (2005) 1189–1196
ELECTROCHIMICA Acta
www.elsevier.com/locate/electacta

Studies of phase composition of Zn–Ni alloy obtained in acetate-chloride electrolyte by using XRD and potentiodynamic stripping

A. Petrauskas*, L. Grincevičienė, A. Češūnienė, R. Juškėnas

Institute of Chemistry, Electrochemistry of Metals, A. Goštauto 9, LT-01108 Vilnius, Lithuania

Received 24 March 2004; received in revised form 26 May 2004; accepted 31 July 2004
Available online 11 September 2004

Abstract

The phase composition of Zn–Ni alloy electrodeposited in acetate-chloride electrolyte has been studied as a function of $ZnCl_2$ concentration and cathodic current density (i_c) by the potentiodynamic stripping and XRD methods. It appeared to be dependent only on the Zn/Ni ratio in the alloy, irrespective of whether the result was attained by varying the cathodic current density or by changing the $[Zn^{2+}]/[Ni^{2+}]$ ratio in electrolyte. A Zn–Ni alloy dissolving in the potential range of i_a peak D can be obtained by the method of cyclic voltammetry. This phase is a compact black coating. It has been determined by potentiodynamic stripping that pure Ni oxidizes only in the range of positive potentials, while Zn–Ni alloy containing some quantity of Zn oxidizes in the range of negative potentials. It was determined that the preciser data of potentiodynamic stripping were obtained in electrolyte containing Cl^- ions. Zn–Ni alloy can be chromated only in the case when the η-phase makes up a sufficiently large portion of Zn–Ni alloy.

Keywords: Electrodeposition; Zn–Ni coatings; Acetate-chloride electrolyte; Stripping

1. Introduction

The investigation of the mechanism of Zn–Ni codeposition has been carried on since 1963 when Brenner [1] thoroughly described anomalous codeposition of Zn and Ni. Extensive studies of Zn–Ni deposition in electrolytes containing ammonia ions have shown that normal or anomalous codeposition takes place depending on the value of potential [2,3] or cathodic current [4]. The authors [3] highlighted three ranges of metal deposition. In the first range of small potentials values (from −0.700 to −0.800 V) the coating contains ≥95 wt.% Ni. In the second range of intermediate potential values the alloy contains approximately 75 wt.% Ni and the cathodic current efficiency of the alloy drops to its lowest value. In the third range of high potential values (from −1.04 to −1.12 V) the quantity of Ni decreases from 45 to 15 wt.% with increase in the potential value and the γ-phase is dominant in the alloy.

Investigation of this phenomenon is important not only from the theoretical but also from practical point of view. It has been known [4–7] that the electrodeposited Zn–Ni alloys containing 10–15 wt.% Ni exhibit a much higher corrosion resistance than the coatings of pure Zn, though they are also distinguished for their anodic protection with respect to Fe. It is believed that Zn–Ni alloys are of optimum composition when they contain 13 wt.% Ni [7]. At present, black Zn–Ni alloys are being applied more and more frequently for decorative finishing of articles.

The mechanism of Zn–Ni codeposition has been investigated in various sulphate [4,2], chloride electrolytes [8,9,3,10], with and without ammonium ions while acetate-chloride electrolytes are much less investigated [7,11]. It has been determined that anticorrosive and physical–mechanical properties of Zn–Ni alloy coatings depend on their phase composition. That is why the studies of phase composition of Zn–Ni alloys by the XRD and potentiodynamic

* Corresponding author. Tel.: +370 5 2612483; fax: +370 5 2617018.
E-mail address: acenin@ktl.mii.lt (A. Petrauskas).

0013-4686/$ – see front matter © 2004 Elsevier Ltd. All rights reserved.
doi:10.1016/j.electacta.2004.07.044

stripping methods have attracted the particular attention [4–6,8,9,3,12–15]. In electrolytic Zn–Ni alloy coatings η-, α- and γ-phases can be detected, while β- and δ-phases of Zn–Ni alloy can be obtained by the pirometallurgical method [4] but they have not been detected in electrodeposited coatings. However, some authors claim, that δ-phase in electrodeposited Zn–Ni alloys was also detected [16,13,10]. It has been found by the potentiodynamic stripping method that there are four typical i_a peaks A–D of anodic dissolution on the potentiodynamic curves (PDC). Peak A is attributed to the anodic dissolution of Zn from the most electrochemical active the η-phase (1% Ni solution in zinc). Some authors [8,14,15] observed i_a peak A as a double, therefore, they claimed that during stripping in this peak the compact γ-phase, which oxidizes at i_a peak C can be formed from a non-compact γ′-phase. Peak B is attributed to Zn dissolution from α-phase. The majority of authors consider i_a peak C as Zn dissolution from the γ-phase, while i_a peak D is unambiguously attributed to anodic dissolution of porous Ni which left after Zn oxidation from η-, α- and γ-phases.

In our previous works it has been determined that under the relevant deposition conditions black decorative coatings of Zn–Ni alloy in acetate-chloride electrolyte without special additives can be deposited. The thickness of these coatings is proportional to the deposition time. Acetate-chloride electrolyte was chosen as an object for our studies owing to its considerable promise for industry.

The aim of this work was to investigate the phase composition of Zn–Ni alloys electrodeposited in acetate-chloride electrolyte as a function of i_c and the $[Zn^{2+}]/[Ni^{2+}]$ ratio by the potentiodynamic stripping and XRD methods.

2. Experimental

Potentiodynamic studies were performed with a potentiostat PI 50-1 in a thermostatic electrochemical cell ISE-2 on a Pt electrode with an area of 1 cm^2. The nickel foil was used as an anode. The anode was separated from the cathode by a diaphragm. To prepare solutions the following salts were used: $Ni(CH_3COO)_2{\cdot}4H_2O$; $ZnCl_2$; KCl; CH_3COOH; H_3BO_3; $MgSO_4{\cdot}7H_2O$. All the used reagents were at least of pro analysis grade.

The Zn–Ni alloys were deposited in electrolyte I (Table 1) with various concentrations of $ZnCl_2$ for experiments under galvanostatic or cyclic voltammetry conditions.

Potentiodynamic stripping of Zn–Ni alloy was performed in electrolyte I or electrolyte II (Table 1).

Table 1
Composition of the electrolytes

Concentration of electrolyte I, c (mol dm^{-3})	$Ni(CH_3COO)_2{\cdot}4H_2O$: 0.56; KCl: 0.91; H_3BO_3: 0.5
Concentration of electrolyte II, c (mol dm^{-3})	$MgSO_4{\cdot}7H_2O$: 0.5; H_3BO_3: 0.5

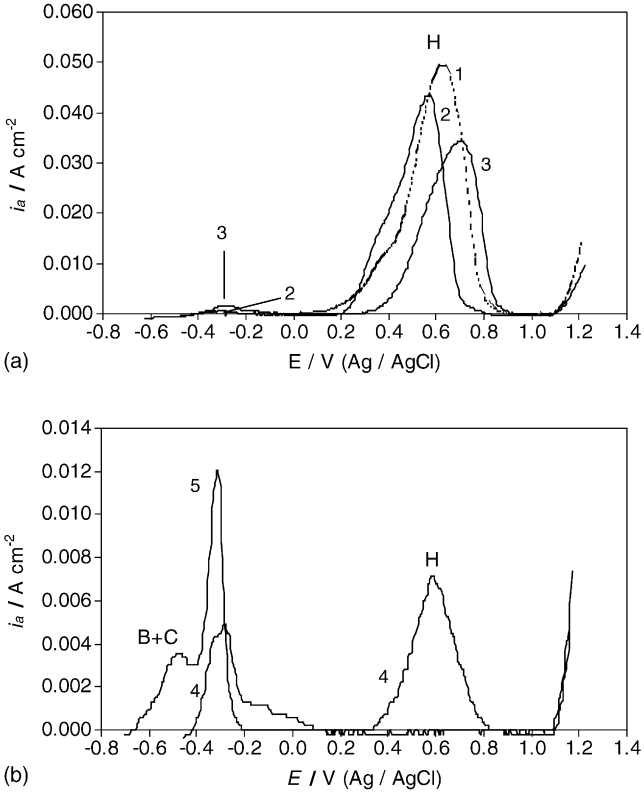

Fig. 1. Potentiodynamic stripping (scan rate = 5 mV s^{-2}) response in electrolyte I of Zn–Ni alloys obtained in electrolyte I with various $ZnCl_2$ concentrations (mol dm^{-3}): (1) 0.0; (2) 0.0037; (3) 0.0047; (4) 0.0055; (5) 0.0073. Time of electrodeposition t = 360 s; i_c = 0.010 A cm^{-2}. t = 20 °C; pH 5. Zn wt.% in alloy: (1) 0.0; (2) 3.5; (3) 10.2; (4) 15.9; (5) 28.9.

Deposition of Zn–Ni alloy coatings was performed at pH 5. The rate of potential scan was v = 5 mV s^{-1}. All the data of potentiodynamic studies are presented in respect to the saturated silver chloride electrode.

An X-ray diffraction (XRD) investigation of Zn–Ni electrodeposits was carried out using an X-ray diffractometer D8 (Bruker AXS). Cu Kα radiation and a continuous scan mode with a scan rate of 1° min^{-1} were used.

The content of Zn and Ni in the alloy was determined by means of electron probe microanalysis with a microanalyser JXA-50A (JEOL).

An atomic force microscope (AFM) SPM Explorer (ThermoMicroscope) was used to determine the average surface roughness of Zn–Ni alloy.

3. Results and discussion

3.1. Stripping in chloride electrolyte

Fig. 1 shows potentiodynamic stripping response in electrolyte I of electrodeposited Ni and Zn–Ni alloys. The PDC of coating obtained in electrolyte I without $ZnCl_2$ exhibits a typical i_a peak H which is attributed to dissolution of pure Ni in

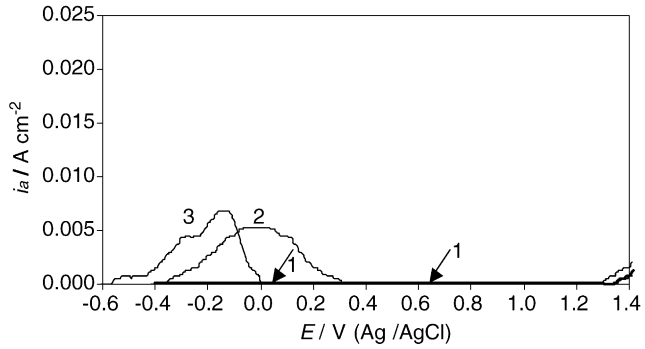

Fig. 2. Potentiodynamic stripping (scan rate = 5 mV s^{-2}) response (in electrolyte II) of Zn–Ni alloys obtained in electrolyte I with different concentrations of $ZnCl_2$ (mol dm^{-3}): (1) 0.0; (2) 0.0055; (3) 0.0073. t = 360 s; i_c = 0.010 A cm^{-2}. t = 20 °C; pH 5. Zn wt.% in alloy: (1) 0.0; (2) 15.9; (3) 28.9.

the range of positive potentials (Fig. 1a, curve 1). The Zn–Ni alloy obtained in electrolyte I containing 0.0037 mol dm^{-3} $ZnCl_2$ has 3.5 wt.% Zn, PDC shows a high i_a peak H attributed to dissolution of pure Ni (Fig. 1a, curve 2) and very low i_a peak also appears in the range of negative potentials (from −0.4 to −0.2 V). After the concentration of $ZnCl_2$ in the electrolyte was increased up to 0.0047 mol dm^{-3}, 10.1 wt.% Zn was found in the alloy, but i_a peak of Ni dissolution dominates in PDC while in the range of negative potentials i_a peak somewhat increases (Fig. 1a, curve 3). When the electrolyte contains 0.0055 mol dm^{-3} $ZnCl_2$ the quantity of Zn in the alloy increases up to 15.9 wt.%, and PDC shows two i_a peaks (Fig. 1b, curve 4). An i_a peak of Zn dissolution from its solid solution of uncertain concentration in nickel (α-phase) manifests itself in the range of negative potentials (from −0.4 to −0.2 V), and i_a peak H of pure Ni dissolution emerges in the range of positive potentials (from 0.4 to 0.8 V).

After concentration of $ZnCl_2$ in electrolyte was increased up to 0.0073 mol dm^{-3}, the quantity of Zn in the alloy reached 28.9 wt.% and PDC did not exhibit i_a peak of Ni dissolution, but there was just i_a peak of Zn–Ni alloy dissolution i_a peaks B + C and D (Fig. 1b, curve 5). This suggests that Zn–Ni alloy electrodeposited under these conditions does not contain phase of pure Ni therefore anodic dissolution of all the phases can occur in the range of negative potentials E < 0.0 V.

3.2. Stripping in sulphate electrolyte

The data presented above were obtained in electrolyte I containing 0.91 mol dm^{-3} KCl, while Zn–Ni alloy was dissolved under conditions when dissolution of Ni was stimulated by Cl^- ions. In Fig. 2 the curves of potentiodynamic stripping response in electrolyte II (sulphate) are presented. Under these conditions while potential was swept from the potential of pure Ni exhibited in studied electrolyte up to $E \leq$ 1.2 V, pure Ni was not dissolved and PDC did not exhibit any i_a peaks up to evolution of O_2 at $E \geq$ 1.3 V (Fig. 2, curve 1).

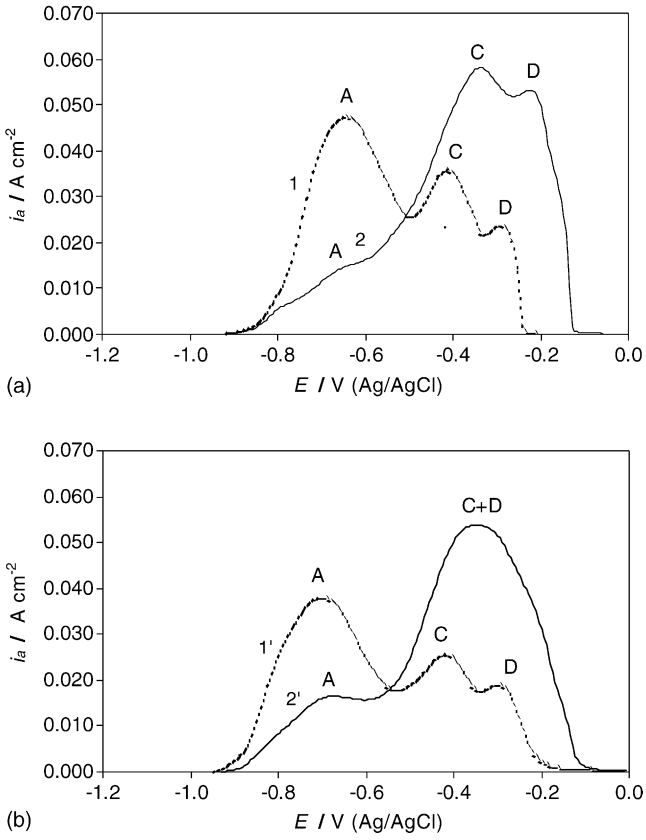

Fig. 3. Potentiodynamic stripping (scan rate = 5 mV s^{-2}) response of the Zn–Ni alloy obtained in electrolyte I with 0.22 mol dm^{-3} of $ZnCl_2$: (a) electrolyte I; (b) electrolyte II. For 1 and 1′ i_c = 0.010 A cm^{-2}; t = 360 s (Zn wt.% = 88.1); for 2 and 2′ i_c = 0.020 A cm^{-2}; t = 180 s (Zn wt.% = 84.5). t = 20 °C; pH 5.

When potentiodynamic stripping of Zn–Ni alloy (Zn = 15.9 wt.%) obtained in electrolyte I with 0.0055 mol dm^{-3} $ZnCl_2$ was performed in sulphate electrolyte, the PDC showed a rather broad i_a peak with a vague top at 0.0 V in

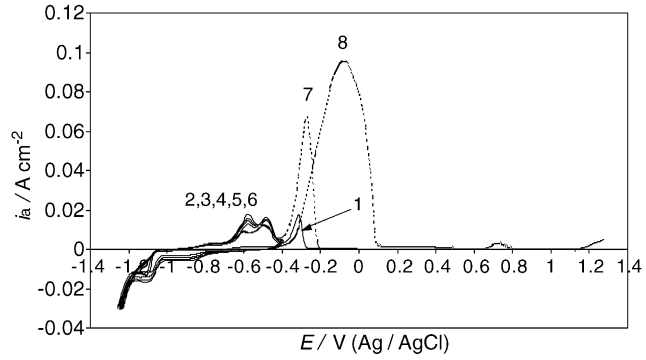

Fig. 4. Cyclic voltammograms (v = 5 mV s^{-1}) of Zn–Ni alloys obtained in electrolyte I with 0.073 mol dm^{-3} $ZnCl_2$ on Pt electrode. Curve 1: the first cycle from Pt potential 0.3 to −1.25 V and back to 0.0 V. Curve 2: the second cycle from 0.0 to −1.25 V and back to −0.4 V. Curves 3–6: the third to sixth cycles from −0.4 to −1.25 V and back to −0.4 V. Curve 7: the seventh cycle from −0.4 to −1.25 V and back to 0 V. Curve 8: 26th cycle from −1.25 to 1.3 V (after 25 cycles from −1.25 to −0.4 V and back to −1.25 V). t = 20 °C; pH 5.

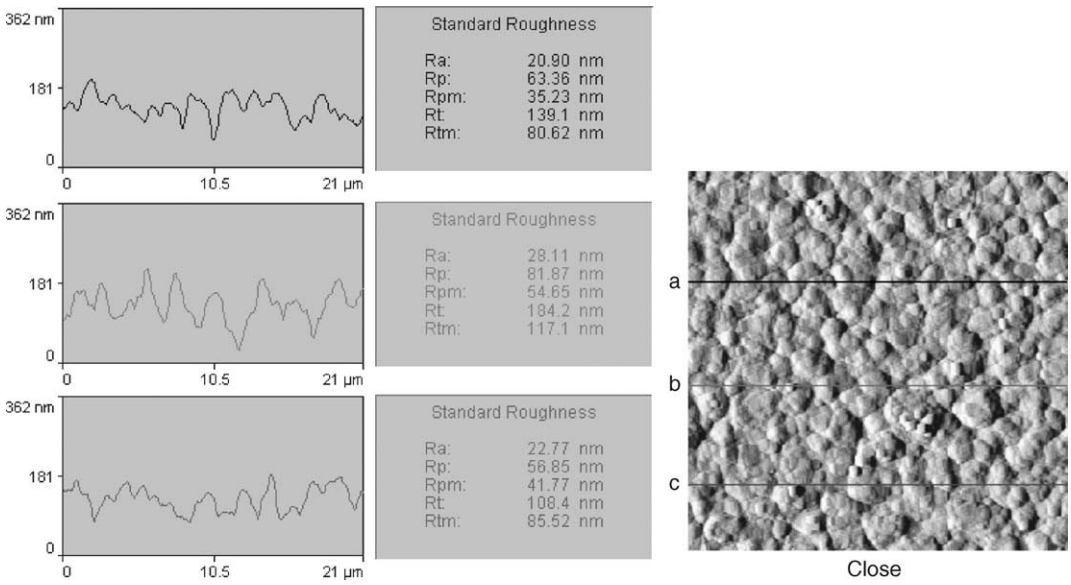

Fig. 5. AFM picture of Zn–Ni alloy obtained on Pt electrode (area 1 cm^2) under the same conditions as in Fig. 4, Curve 8 only after 190 cycles; 5000×. The mean value of the average roughness of the Pt surface, $\bar{R}_a = 4.78$ nm.

the potential range from −0.4 to 0.4 V (Fig. 2, curve 2). In PDC recorded for Zn–Ni alloy (Zn = 28.9 wt.%) obtained in electrolyte I with 0.0073 mol dm^{-3} $ZnCl_2$ just i_a peak manifested itself in the range of the negative potentials (Fig. 2, curve 3).

Fig. 3 presents potential stripping response in chloride and sulphate electrolytes of Zn–Ni alloys obtained in electrolyte with 0.22 mol dm^{-3} $ZnCl_2$. The alloys contained depending on i_c—88.1 and 84.5 wt.% Zn. Potentiodynamic dissolution of the coatings containing 88.1 wt.% Zn, in both the chloride and sulphate electrolytes resulted in PDCs which had nearly analogous i_a peaks A, B + C and D (Fig. 3, curves 1 and 1′). PDCs of the coatings containing a lower quantity (84.5 wt.%) of Zn recorded in the chloride electrolyte showed i_a peaks A, B + C and D (Fig. 3a, curve 2), while in sulphate electrolyte i_a peaks B + C and D merged into one (Fig. 3b, curve 2′). Therefore, in our opinion, potentiodynamic stripping should be performed only in electrolytes with Cl^- ions, because in a sulphate electrolyte the data were distorted by passivation of Ni.

3.3. *Formation of Zn–Ni alloy which dissolves during potentiodynamic stripping in the potential range of i_a peak D*

The data presented in Fig. 1 show, that pure Ni can dissolve in the range of positive potentials, but according to references i_a peak D is also attributed to Ni dissolution from the porous Ni matrix. However, some authors claim that during stripping the Ni/Zn ratio in alloy varies as Zn is removed from the most active η- and γ-phases, therefore, phase transition can take place and α- [14] or β-[15] phases can be formed.

To study processes occurring in the potential range (from −0.35 to 0.0 V) of i_a peak D an experiment in order to accumulate a large quantity of Zn–Ni alloy that could further dissolve only in i_a peak D was performed. For this purpose the alloy was deposited by cyclic polarization of Pt electrode, i.e. by sweeping E from −1.25 to −0.4 V. Under these conditions with decrease in E up to −1.25 V, all the Zn–Ni alloy phases can be deposited, when E is increased up to −0.4 V (the beginning of i_a peak D) Zn is removed from η-, α- and γ-phases leaving on the electrode only a newly formed phase, dissolving at $E > -0.4$ V (at i_a peak D). As is seen in Fig. 4, curve 1, i_a peak D obtained after the first cycle is small size, while after 7 or 25 cycles (curves 7 and 8 respectively) it is many times larger than the former. The Zn–Ni alloy coating obtained by this method is black, compact and fine-grained (Fig. 5).

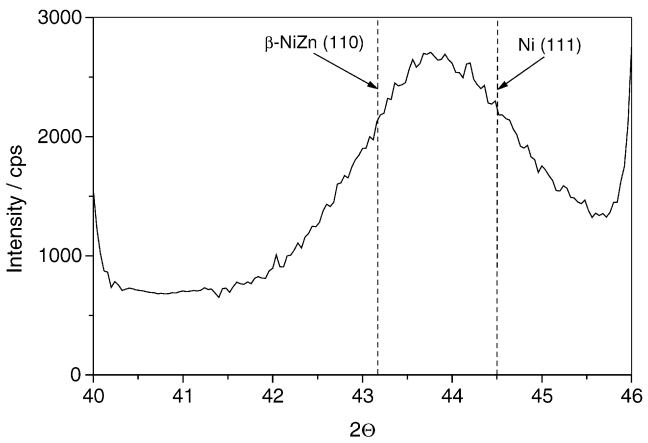

Fig. 6. XRD pattern of Zn–Ni phase formed during cycling for 6 h.

Table 2
Zn quantity (wt.%) in Zn–Ni alloy as a function of $ZnCl_2$ concentration in electrolyte I and i_c of electrodeposition: t = 20 °C; pH 5

i_c (A cm^{-2})	$ZnCl_2$ (mol dm^{-3})			
	0.029	0.058	0.11	0.22
0.020	18.8 (1)[a]	43.6 (5)	56.0 (6)	–
0.010	35.9 (4)	58.0 (7)	77.5 (9)	–
0.005	19.2 (2)	33.2 (3)	60.7 (8)	88.7 (10)

[a] The numbers of XRD patterns (Fig. 7) and potentiodynamic stripping PDC (Fig. 9; curves 1–3 and 7–10) given in brackets help to arrange them in order of increasing Zn quantity (wt.%) in Zn–Ni alloy.

Analysis of the coating obtained by this method after 190 cycles have shown the presence of 42.4 wt.% Zn and 57.6 wt.% Ni in the alloy. This composition is close to that of the β-phase (NiZn). The 15.2 wt.% excess of Ni could support the statement that at the first i_a peaks only Zn dissolution from different phases of Zn–Ni alloy takes place and Ni accumulates on the electrode. It could be expected that during anodic dissolution of Zn–Ni alloy accumulated on the electrode under the cycling double peak of i_a attributed to Zn and Ni will manifest itself on PDC. Because of this during experiment the number of cycles was varied from 1 to 80, however, in all cases during anodic dissolution only a single i_a peak was observed, which might be attributed to the anodic dissolution of the β-phase formed during cycling. Moreover, this Zn–Ni alloy phase accumulated during cycling and comprising 42 wt.% Zn actively dissolves in diluted (10%) HCl. This was the reason why XRD studies were performed.

Fig. 6 shows a fragment of the pattern indicating that maximum the experimental peak is located between positions of the XRD peaks corresponding to β-NiZn and pure Ni phases. It could mean that Zn–Ni deposit obtained by cycling in potential range from −1.25 to −0.4 V presents β-NiZn phase with increased Ni content (there is 40% of Zn only according to elemental analysis). On the other hand it could mean that a solid solution of Zn in nickel was formed during cycling. About 10% of zinc must be in the other phase—amorphous pure zinc or ZnO—in the latter case.

The data obtained suggest (Figs. 4 and 6) that Zn–Ni alloy can be obtained by the cyclic voltammetry method, the latter dissolves in the potential range of i_a peak D.

3.4. Dependence of phase composition of Zn–Ni alloy on Zn content in the alloy

When the relevant deposition conditions of alloy are chosen, it is possible at various i_c and different concentrations of $ZnCl_2$ to deposit Zn–Ni alloys containing the same Zn/Ni ratio in it. For example the Zn–Ni alloys deposited in electrolyte I containing 0.44 mol dm^{-3} $ZnCl_2$ at i_c = 0.40 A cm^{-2} and those deposited in electrolyte I containing 0.15 mol dm^{-3} $ZnCl_2$ at i_c = 0.0025 A cm^{-2} appeared to contain nearly the same quantity of Zn, i.e. 85.7 and 85.0 wt.%, respectively. Potentiodynamic stripping of these coatings resulted in analogous PDCs. That is why the specimens of Zn–Ni alloys obtained at different i_c and at various $ZnCl_2$ concentrations were prepared (Table 2).

Fig. 7 shows dependence of phase composition on Zn quantity in Zn–Ni deposit. At low zinc quantities (∼19 wt.%) the deposit consists of nickel and nickel rich α-phase, which is inhomogeneous with respect to the zinc concentration. Fig. 7a presents a fragment of the XRD pattern no. 1 in Fig. 7. Deconvolution of the peak at 2Θ of ∼76° shows that it presents an overlap of two peaks (dashed curves): maximum of the first peak correspond to d value of 0.1264 nm and can be attributed to α-Ni phase and the second one with d value of 0.1247 nm belongs to pure Ni phase.

In different crystallites of α-phase the Zn quantity can vary in the range from 0 to 30 wt.% (Zn dissolution limits in nickel). As zinc quantity reaches ∼33 wt.% Ni–Zn electrodeposit is composed of three phases: Ni, α-Ni–Zn and γ-Ni_5Zn_{21}. A negligible increase in Zn quantity (from 33.2 to 35.9 wt.%) significantly increases the content of γ-Ni_5Zn_{21} phase. However, this may be caused by the different current densities used. When zinc quantity reaches 56 wt.% a pure nickel phase becomes undetectable by XRD, though a small quantity of Ni–Zn α-phase remains. As Zn amounts 60 wt.% Ni–Zn α-phase becomes undetectable, as well. The quantity of Ni reaches 33.5 wt.% and it is much higher than that required for the formation of γ-Ni_5Zn_{21} phase (i.e. ∼18 wt.%). Other authors [17] state that Zn–Ni η-phase (solid solution of up to 6 wt.% of Ni in zinc) was formed, however, we did not detect such a phase. On the other hand, the same authors state that a Zn solid solution in γ-Ni_5Zn_{21} phase was formed and it caused an increase in lattice parameter (from 0.892 to 0.894 nm). We observed the inverse effect i.e. lattice parameter a of γ-Ni_5Zn_{21} phase decreased when nickel content was higher than 15–18 wt.% (Fig. 8). The assumption that nickel atoms in the lattice of γ-Ni_5Zn_{21} substitute some Zn atoms could explain why any Ni or α-Ni–Zn phases are not observed despite the Ni excess in the deposit.

A small quantity of ZnO was detected in some samples electrodeposited under a current density of 0.010 A cm^{-2} (Fig. 7b, sample no. 8). Fig. 7b shows XRD pattern no. 8 in Fig. 7 giving evidence that ZnO is present in the electrodeposit of Zn–Ni alloy containing 60.7% of Zn. Intensities of the diffracted X-rays are given in logarithmic scale to make ZnO peaks visible more definitely. It should be noted that ZnO was found in the deposits containing the γ-Ni_5Zn_{21} phase. Other authors [12], who studied Zn–Ni electrodeposition from ammonium chloride solution, assert that ZnO incorporates into

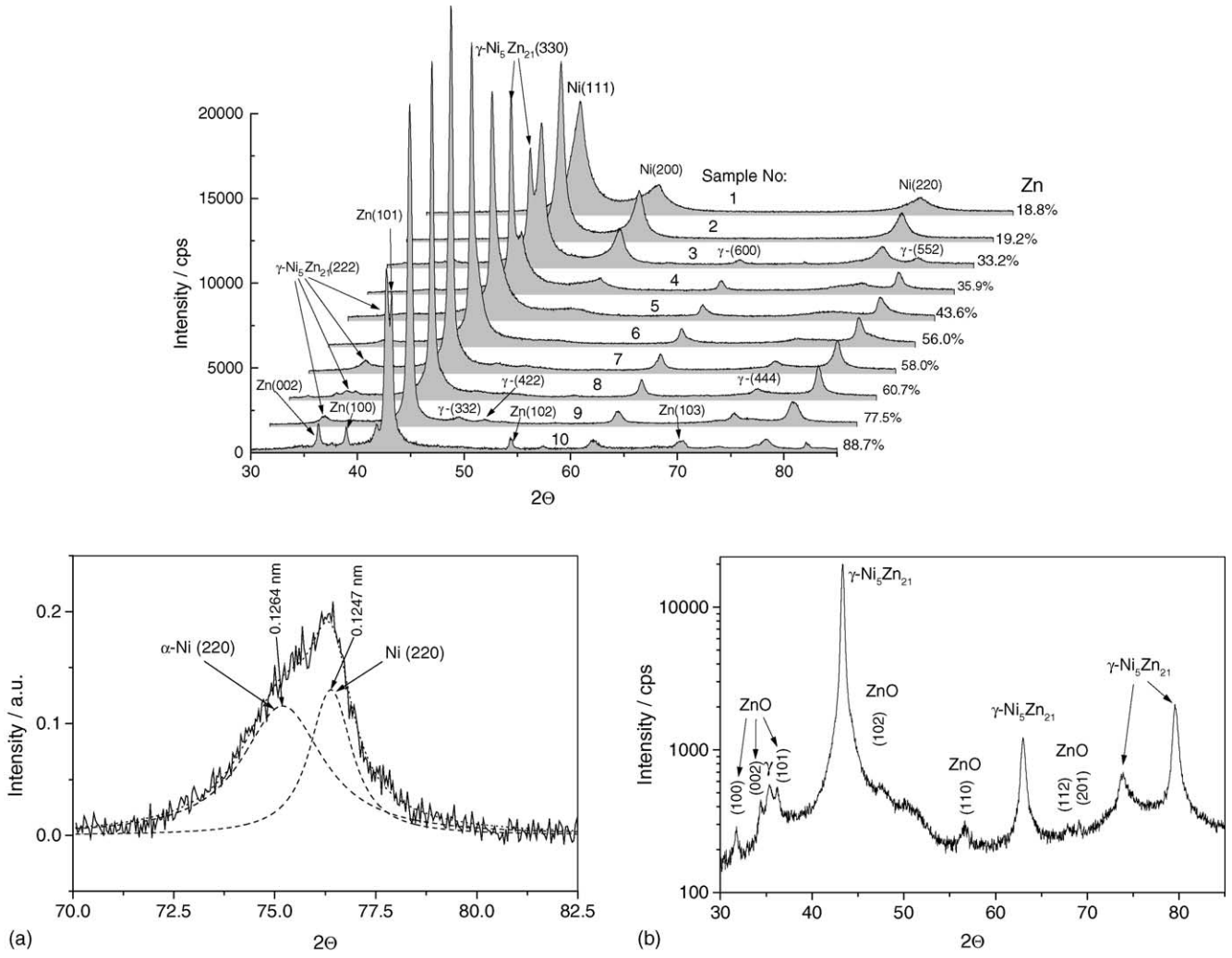

Fig. 7. XRD patterns of Ni–Zn deposits with various Zn content. The deposition conditions for each sample are presented in Table 1; Cu Kα radiation: (a) a fragment of the XRD pattern no. 1 and (b) XRD pattern no. 8 for Zn–Ni electrodeposited alloy containing 60.7% of Zn.

deposit when the α-Ni–Zn phase is formed. The formation of ZnO was caused by increase in pH in the vicinity of the cathode surface due to intensive hydrogen evolution. According to these authors hydrogen overvoltage is much higher on the γ-Ni_5Zn_{21} phase than that on the α-Ni–Zn phase. However, it has been determined by other authors that it is γ-Ni_5Zn_{21} phase that is distinguished for a high catalytic activity in hydrogen evolution [18]. When Zn quantity in the Zn–Ni alloy amounts 88.7% XRD peaks corresponding to pure Zn phase appear on the pattern (Fig. 7, pattern no. 10). These peaks can be attributed to Zn–Ni η-phase containing ≤1% of nickel as well.

The stripping method is more advisable than XRD as it makes it possible to quantitatively estimate the phase composition of Zn–Ni alloy. The only problem being that α-phase of Zn–Ni alloy (solid zinc solution in nickel) is not of constant composition, as Zn quantity in it can vary ≤30 wt.% and the oxidation of this phase can occur in a wide potential range. i_a peak B of Zn dissolution from the α-phase often overlaps i_a peak C of Zn dissolution from the γ-phase Because of this reason the stripping data should be supported by the data of XRD studies.

Fig. 9a, curve 1 shows a representative example of the case when all peaks overlap during potentiodynamic stripping. In this case only on the basis of the data of XRD studies one can assert that this PDC reflects Zn dissolution from the α-phase of uncertain composition. However, it still remains unclear if it is Zn dissolution from the α-phase or it is the dissolution of the α-phase itself. This i_a peak is shifted 55 mV in the direction of negative potentials in relation to i_a peak D. If assume that i_a peak D is attributed to Ni matrix dissolution, then in the Fig. 9a, curve 1 Ni dissolution was not observed.

The data of XRD studies have shown that the γ-phase appears in the alloy only when Zn content reached 33.2 wt.% (Fig. 7, curve 3), meanwhile there are two anodic peaks B + C and D on the PDC of alloy, containing 19.2 wt.% Zn.

i_a peak B + C is attributed to the Zn dissolution from the α-and γ-phases, however, XRD patterns show no of the presence γ-phase in Zn–Ni alloy. It suggests that the

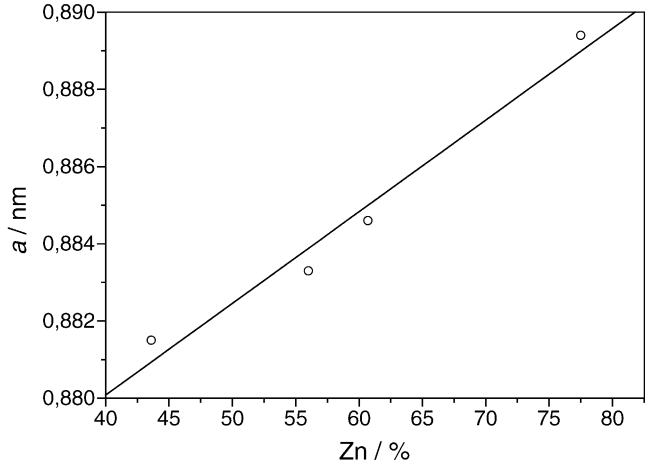

Fig. 8. Dependence of γ-Ni_5Zn_{21} phase lattice parameter *a* on Zn quantity (wt.%) in Ni–Zn deposit.

potentiodynamic stripping method better represents phase composition of Zn–Ni alloy.

With further increase in Zn quantity in the alloy from 58.0 to 77.5 wt.% (Fig. 9b, curves 7 and 9), the i_a peak B + C in PDC increases from 0.037 to 0.057 A cm^{-2}. This can be explained by increase in the quantity of the γ-phase in Zn–Ni alloy. The PDC of Zn–Ni alloy, deposited from electrolyte I with 0.022 mol dm^{-3} $ZnCl_2$ at i_c = 0.005 A cm^{-2} (88.7 wt.% Zn) (Fig. 9c, curve 10) is quite different from PDCs represented in Fig. 9a and b. In this case, the PDC exhibits i_a peak A which is attributed to the dissolution of Zn from the η-phase (Fig. 9c, curve 10). This also was confirmed by XRD pattern (Fig. 7, pattern no. 10).

Acidic chromating solution containing 0.31 mol dm^{-3} Cr^{6+} and 1.7 ml dm^{-3} H_2SO_4 (d = 1.84 g/cm^3) is used for passivation of Zn coatings in the industry. During passivation a layer of Zn coating partially dissolved, and passivating film of $Cr(OH)_3$ and $Zn(OH)_2$ covered the surface. It has been noticed that Zn–Ni alloys with Ni >20 wt.% and with prevailing the γ-phase did not react with passivation solutions and, therefore, a passivating rainbow film was not formed on their surface. The sample of Zn–Ni alloy marked as no. 10 contained 88.7 wt.% Zn and large quantity of η-phase (1 wt.% Ni solution in Zn) (Table 2 and Fig. 9c, curve 10, i_a peak A).

After exposure of such alloy to chromating solution for some time, i_a peak A is not observed during potentiodynamic stripping. The reason is that a chromating solution removed Zn from the η-phase, because Ni cannot be dissolved under these conditions. When potentiodynamic stripping is performed after chemical dissolution of the coating a distinct increase in i_a peak B + C is observed. It suggests that under these conditions a transition of the non-compact γ-phase occurs and the quantity of the γ-phase increases. An analogous phenomenon was also observed by the authors of [15]. If assume, that during cycling the Zn–Ni alloy, which can dissolve in the

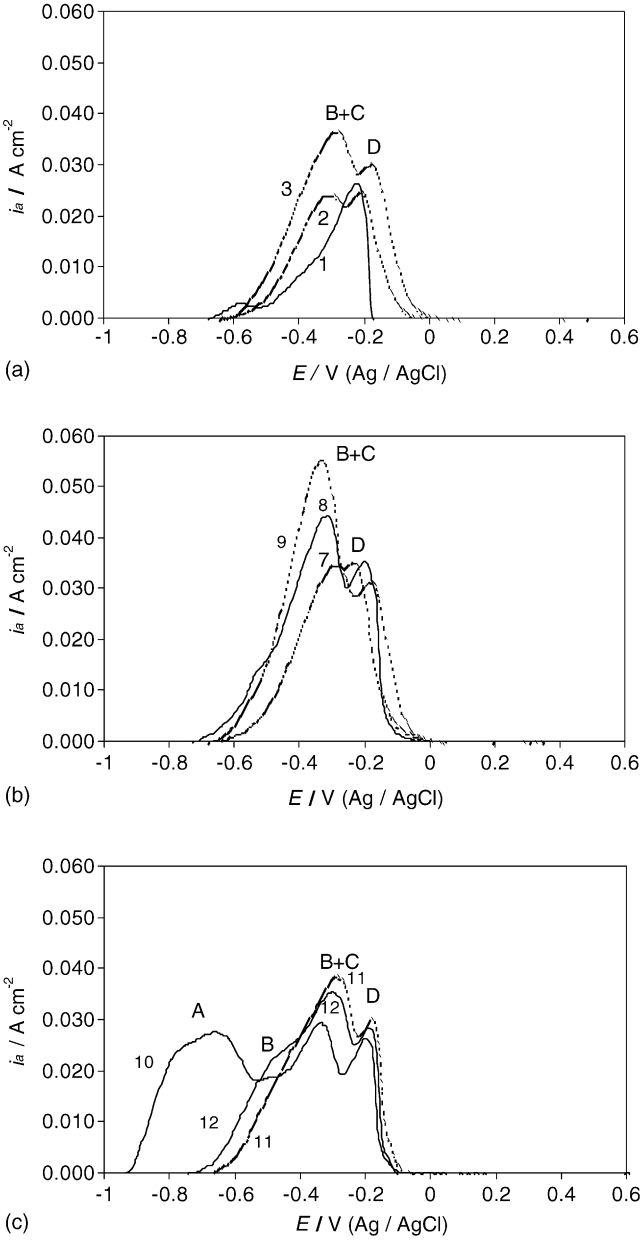

Fig. 9. Curves (1–3 and 7–10) of potentiodynamic stripping (in electrolyte I) response of Zn–Ni alloys deposited in electrolyte I at various $ZnCl_2$ concentrations and various i_c. The conditions of deposition indicated in Table 2. PDC (11; 12) obtained after immersion the sample of Zn–Ni alloy marked as no. 10 into chromating solution containing 0.31 mol dm^{-3} Cr^{6+} and 1.7 ml dm^{-3} H_2SO_4 (d = 1.84 g/cm^3) for 180 and 600 s, respectively; v = 5 mV s^{-1}. t = 20 °C; pH 5.

potential range of i_a peak D, accumulates on the electrode (Fig. 4, curves 7 and 8), the processes occurring in Fig. 9 at i_a peaks D should be assigned to the dissolution of this alloy, but not to the dissolution of pure Ni. Obviously, this assumption requires further investigations; therefore, thorough studies of the processes taking place during potentiodynamic stripping in i_a peaks C and D were scheduled to start in the nearest future.

4. Conclusions

1. It was determined that the preciser data of potentiodynamic stripping were obtained in electrolyte containing Cl^- ions.
2. During potentiodynamic stripping dissolution of pure Ni occurs only in the range of positive potentials.
3. It has been assumed that by using the cyclic voltammetry method (from -1.25 to -0.4 V) a considerable quantity of Zn–Ni alloy, which dissolves in the range of potentials of i_a peak D, can be accumulate on the electrode.
4. Phase composition of Zn–Ni alloy depends only on the ratio Zn/Ni in it.
5. Zn–Ni alloy can be chromated only in the case when the η-phase makes up a sufficiently large portion of Zn–Ni alloy.

References

[1] A. Brenner, Electrodeposition of Alloys, vol. 1, Academic Press, New York, 1963, p. 77.
[2] F.J. Fabri Miranda, O.E. Barcia, S.L. Diaz, O.R. Mattos, R. Wiart, Eletrochem. Acta 41 (7–8) (1996) 1041.
[3] F. Elkhatabi, M. Benballa, M. Sarret, C. Müller, Electrochem. Acta 44 (10) (1999) 1645.
[4] D.E. Hall, Plating Surf. Finish 70 (11) (1983) 59.
[5] J. Garcia, J. Barcelo, M. Sarret, C. Müller, J. Pregonas, J. Appl. Electrochem. 24 (1994) 1249.
[6] M. Gavrila, J.P. Millet, H. Mazille, D. Marchandise, J.M. Cuntz, Surf. Coat. Technol. 123 (2000) 164.
[7] E. Beltowska-Lehman, P. Ozga, Z. Swaitek, C. Lupi, Surf. Coat. Technol. 151–152 (2002) 444.
[8] S.S. Swathijaran, J. Electrochem. Soc. 133 (4) (1986) 671.
[9] F. Elkhatabi, M. Sarret, C. Müller, J. Electroanal. Chem. 404 (1) (1996) 45.
[10] Z. Wu, L. Fedrizzi, P.I. Bonora, Surf. Coat. Technol. 85 (3) (1996) 170.
[11] S.S. Abd El Rehim, E.E. Foaud, S.M. Abd El Wahab, H.H. Hassan, Eletrochem. Acta 41 (9) (1996) 1413.
[12] C. Müller, M. Sarret, M. Benballa, Electrochem. Acta 46 (18) (2001) 2811.
[13] J. Stevanovic, S. Gojkovic, A. Despic, M. Obradovic, V. Nakic, Electrochem. Acta 43 (7) (1998) 705.
[14] F. Elkhatabi, G. Barcelo, M. Sarret, C. Muller, J. Electronal. Chem. 419 (1) (1996) 71.
[15] Y.-P. Lin, R. Selman, J. Electrochem. Soc. 140 (5) (1993) 1299.
[16] L. Felloni, R. Fratesi, E. Quadrini, G. Roventi, J. Appl. Electrochem. 17 (3) (1987) 574.
[17] C. Müller, M. Sarret, M. Benballa, J. Eletroanal. Chem. 519 (2002) 85.
[18] C.-C. Hu, C.-H. Tsay, A. Bai, Electrochem. Acta 48 (7) (2003) 907.